

Gelation of Perfluorinated Liquids by *N*-Alkyl Perfluoroalkanamides[†]

Mathew George,[‡] Samuel L. Snyder,[‡] Pierre Terech,[§] and Richard G. Weiss^{*,‡}

Department of Chemistry, Georgetown University, Washington, D.C. 20057-1227, and
Laboratoire Physico-Chimie Moléculaire, UMR 5819 CEA-Grenoble, 17 rue des Martyrs,
38054 Grenoble Cedex 09, France

Received February 9, 2005. In Final Form: March 3, 2005

Gels comprised of low-molecular-mass organic gelators (LMOGs), *N*-alkyl perfluoroalkanamides [F(CF₂)_mCONH(CH₂)_nH; FmNHn], and several perfluorinated liquids are described. The gelation ability of the amides has been compared to that of two analogous alkyl perfluoroalkanoates. The properties of these gels have been correlated with the *N*-alkyl and (to a lesser extent) perfluoroalkyl chain lengths in the FmNHn by X-ray diffraction, polarizing optical microscopy, infrared spectroscopy, and small-angle neutron scattering. The gels are thermally reversible and require generally very low concentrations (<2 wt %) of LMOG. Several of the gels have been stable at room temperature for >1 year, thus far. The incompatibility of the fluorocarbon and hydrocarbon segments causes the LMOGs to aggregate into lamellae within the fibrils that constitute the basic unit of the gel networks. IR spectroscopic studies of these gels indicate that additional ordering within the aggregate units is enforced by intermolecular H-bonding among amide groups.

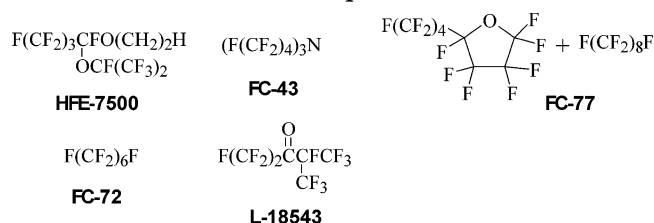
Introduction

Interest in low-molecular-mass organic gelators (LMOGs), the structures of their self-assembled fibrillar networks (SAFINs), and, especially, the properties of the thermally reversible organogels they produce has increased enormously during the last several years.¹ Organogels are formed commonly when an isotropic solution or sol, consisting of a small amount of an LMOG and an organic liquid, is cooled below its characteristic gelation temperature (*T*_g). During this process, the LMOG molecules aggregate into fibers, strands, tapes, and other elongated objects, joined at “junction zones”² to form SAFINs that immobilize the liquid component, primarily by surface tension and capillary forces.^{1a,2} The microheterogeneous SAFINs can have a wide variety of structures expressed from the molecular to the micrometer distance scales. The unusual properties of organogels have led to several interesting applications,³ and they can be used as structure-directing agents for inorganic nanoparticles.⁴ Because the LMOG concentration is usually very low, there need be no specific liquid–gelator interactions that

Chart 1. F(CF₂)_mCOX(CH₂)_nH Gelators

FmNHn	FmOHn
m = 7, X = NH, n = 18	m = 11, X = O, n = 3
m = 11, X = NH, n = 3	m = 11, X = O, n = 18
m = 11, X = NH, n = 4	
m = 11, X = NH, n = 6	

Chart 2. Perfluorinated Liquids for Gelation Studies



affect the vast majority of the liquid on a molecular scale; the gels are not like clathrates, for instance. Models to describe the stages of aggregation in some organogels have been presented recently.^{1f,5}

Gels of *N*-alkyl perfluoroalkanamides, FmNHn (Chart 1), in perfluorinated liquids (Chart 2) are reported here, and their properties are compared to those of gels with two analogous esters, FmOHn, as the gelators. Gels of these LMOGs in different organic liquids, such as hydrocarbons, alcohols, halogenated liquids, silicone oil,⁶ and polar aprotic liquids, have been investigated previously.⁷ The molecular structures of these LMOGs contain “incompatible” segments—fluorocarbons and hydrocarbons are immiscible below a certain temperature—and the

* Author for correspondence. Fax: (202) 687-6209. Telephone: (202) 687-6013. E-mail: weissr@georgetown.edu.

[†] Part of the Bob Rowell Festschrift special issue.

[‡] Georgetown University.

[§] Laboratoire Physico-Chimie Moléculaire.

(1) (a) Terech, P.; Weiss, R. G. *Chem. Rev.* **1997**, *97*, 3133–3159. (b) Abdallah, D. J.; Weiss, R. G. *Adv. Mater.* **2000**, *12*, 1237–1247. (c) van Esch, J. H.; Feringa, B. L. *Angew. Chem., Int. Ed.* **2000**, *39*, 2263–2266. (d) Shinkai, S.; Murata, K. *J. Mater. Chem.* **1998**, *8*, 485–495. (e) Terech, P.; Weiss, R. G. In *Surface Characterization Methods*; Milling, A. J., Ed.; Marcel Dekker: New York, 1999; p 286. (f) Weiss, R. G.; Terech, P., Eds. *Molecular gels. Materials with Self-Assembled Fibrillar Networks*; Springer: Dordrecht, 2005 (expected).

(2) Terech, P.; Furman, I.; Weiss, R. G. *J. Phys. Chem.* **1995**, *99*, 9558–9566.

(3) (a) Derossi, D.; Kajiwar, K.; Osada, Y.; Yamauchi, A. *Polymer gels: Fundamentals and Biomedical Applications*; Plenum Press: New York, 1991. (b) Bhattacharya, S.; Ghosh, Y. K. *Chem. Commun.* **2001**, 185–186. (c) Vidal, M. B.; Gil, M. H. *J. Bioact. Compat. Polym.* **1999**, *14*, 243–257. (d) Pozzo, J.-L.; Clavier, G. M.; Desvergne, J.-P. *J. Mater. Chem.* **1998**, *8*, 2575–2577. (e) de Loos, M.; van Esch, J.; Stokroos, L.; Kellogg, R. M.; Feringa, B. L. *J. Am. Chem. Soc.* **1997**, *119*, 12675–12676. (f) Jung, J. H.; Ono, Y.; Shinkai, S. *Chem.—Eur. J.* **2000**, *6*, 4552. (g) Terech, P. *Ber. Bunsen-Ges. Phys. Chem.* **1998**, *102*, 1630–1643.

(4) (a) Kobayashi, S.; Hamasaki, N.; Suzuki, M.; Kimura, M.; Shirai, H.; Hanabusa, K. *J. Am. Chem. Soc.* **2002**, *124*, 6550–6551. (b) Jung, J. H.; Ono, Y.; Shinkai, S. *Angew. Chem., Int. Ed.* **2000**, *39*, 1862–1865. (c) Jung, J. H.; Ono, Y.; Hanabusa, K.; Shinkai, S. *J. Am. Chem. Soc.* **2000**, *122*, 5008–5009. (d) Ono, Y.; Nakashima, K.; Sano, M.; Hojo, J.; Shinkai, S. *J. Mater. Chem.* **2001**, *11*, 2412–2419. (e) Jung, J. H.; Ono, Y.; Shinkai, S. *Chem.—Eur. J.* **2000**, *6*, 4552–4557.

(5) Aggeli, A.; Nyrkova, I. A.; Bell, M.; Harding, R.; Carrick, L.; McLeish, T. C. B.; Semenov, A. N.; Boden, N. *Proc. Natl. Acad. Sci. U.S.A.* **2001**, *98*, 11857–11862.

(6) Tetramethyltetraphenyltrisiloxane (Dow silicone oil 704).

(7) George, M.; Snyder, S. L.; Glinka, C. J.; Terech, P.; Weiss, R. G. *J. Am. Chem. Soc.* **2003**, *125*, 10275–10283.

cross-sectional areas of the $-(\text{CH}_2)_n-$ and $-(\text{CF}_2)_m-$ segments are 18.5 and 28.3 Å², respectively,⁸ making their isomorphous substitution into each other's solid matrixes very difficult.

Molecules of FmHn into which an ester group has been inserted cannot undergo intermolecular H-bonding. Dipole–dipole forces are the strongest interactions between their ester groups. Both intermolecular H-bonding and dipole–dipole interactions are available between secondary amide groups such as the ones inserted into FmHn.⁹ The use of amide groups is a common strategy to enhance the gelating ability of LMOGs.¹⁰ We find that very low concentrations of some of the FmNHn are able to gelate a wide variety of perfluorinated liquids. Here, the gelation temperatures and periods of stability of the gels are correlated with data from IR, optical microscopy, X-ray diffraction, and small-angle neutron scattering (SANS) to identify the factors responsible for the enhanced gelation of the perfluorinated liquids by the amides. This information should provide a basis for the design of other gelators when they are needed to deliver perfluorinated liquids for specific purposes, such as in electronics manufacturing,¹¹ heat transfer,¹² lithography,¹³ lubrication,¹⁴ and even fire retardation.¹⁵

Typically, perfluorinated molecules have very strong covalent bonds, very weak intermolecular interactions, and very low surface free energies.¹⁶ As a result, they exhibit several properties—exceptional thermal, chemical and biological inertness, low surface tension, high fluidity, excellent spreading characteristics, low solubility in water, and high gas-dissolving capacities—which make them the materials of choice for many industrial applications. Both as a basic scientific challenge and as a potential extension to methods employed to deliver perfluorinated molecules

for industrial purposes, we sought to develop LMOGs which, at relatively low concentrations, are able to gelate thermoreversibly a wide variety of perfluorinated liquids. Our results demonstrate that the *N*-alkyl perfluoroalkanamides in Chart 1 are more general and better gelators of perfluorinated liquids than any of the LMOGs reported to date.

There are relatively few reported examples of the gelation of perfluorinated liquids by LMOGs. Relatively high concentrations of diblock (perfluoroalkyl)alkane molecules (FmHn; related structurally to our FmNHn) gelate several liquids,^{17,18} including mixtures of *n*-perfluorooctane and isooctane,¹⁹ and perfluorodecaline.²⁰ Fluorinated surfactants and ionomers are known to gelate a variety of liquids including functionalized perfluoroalkanes containing 1–20% of water.²¹ Hexafluorobenzene has been gelated by 12-hydroxyoctadecanoic acid.²² Some partially fluorinated LMOGs containing semifluorinated aralkyl amide and glycolipid derivatives²³ and a tetrakis-trifluoromethylated stilbene and oligomers end-capped with perfluorinated moieties or attached as pendant groups²⁴ are known to gelate nonfluorinated liquids. In addition, tetra(fluoroalkoxy)silanes can form extremely low-density materials through an uncatalyzed sol–gel process.²⁵

Experimental Section

Instrumentation. Polarized optical micrography (POM) of gels was performed on a Leitz 585 SM-LUX-POL microscope equipped with crossed polars and a Photometrics CCD camera interfaced to a computer. IR spectra were obtained on a Perkin-Elmer Spectrum One FT-IR spectrometer interfaced to a PC. X-ray diffraction (XRD) of samples in thin, sealed capillaries (0.5 mm diameter; W. Müller, Schönwalde, FRG) was performed on a Rigaku R-AXIS image plate system with Cu K α X-rays ($\lambda = 1.540\ 56\ \text{\AA}$) generated with a Rigaku generator operating at 46 kV and 46 mA. Data processing and analyses were performed using Materials Data JADE (version 5.0.35) XRD pattern processing software.²⁶ Molecular calculations of lowest energy conformations and molecular dimensions used the semiempirical Parametric Method 3 (PM3)²⁷ of the HYPERCHEM package, release 5.1 Pro for Windows from Hypercube, Inc.

Small-angle neutron diffraction measurements were obtained on the low-angle diffractometer NG7 at the National Institute

(8) (a) LoNostro, P.; Ku, C. Y.; Chen, S. H.; Lin, J. S. *J. Phys. Chem.* **1995**, *99*, 10858–10864. (b) LoNostro, P. *Adv. Colloids Interface Sci.* **1995**, *56*, 245–287.

(9) Challis, B. C.; Challis, J. A. In *Comprehensive Organic Chemistry: The Synthesis and Reactions of Organic Compounds*; Barton, D. H. R., Ollis, W. D., Eds.; Pergamon Press: New York, 1979; Vol. 2, p 957.

(10) (a) Jokić, M.; Makarević, J.; Žinić, M. *J. Chem. Soc., Chem. Commun.* **1995**, 1723–1724. (b) Makarević, J.; Jokić, M.; Perić, B.; Tomišić, V.; Kojić-Prodić, B.; Žinić, M. *Chem.—Eur. J.* **2001**, *7*, 3328–3341. (c) Luo, X.; Liu, B.; Liang, Y. *Chem. Commun.* **2001**, 1556–1557. (d) Tomioka, K.; Sumiyoshi, T.; Narui, S.; Nagaoka, Y.; Iida, A.; Miwa, Y.; Taga, T.; Nakano, M.; Handa, T. *J. Am. Chem. Soc.* **2001**, *123*, 11817–11818. (e) Suzuki, M.; Yumoto, M.; Kimura, M.; Shirai, H.; Hanabusa, K. *Chem. Commun.* **2002**, 884–885. (f) Makarević, J.; Jokić, M.; Frkanec, L.; Katalenic, D.; Žinić, M. *Chem. Commun.* **2002**, 2238–2239. (g) Frkanec, L.; Jokić, M.; Makarević, J.; Wolsperger, K.; Žinić, M. *J. Am. Chem. Soc.* **2002**, *124*, 9716–9717. (h) Suzuki, M.; Yumoto, M.; Kimura, M.; Shirai, H.; Hanabusa, K. *Chem.—Eur. J.* **2003**, *9*, 348–354.

(11) Lee, S.-H.; Kwon, M.-J.; Park, J.-G.; Kim, Y.-K.; Shin, H.-J. *Surf. Coat. Technol.* **1999**, *112*, 48–51.

(12) (a) Bergles, A. E.; Bar-Cohen, A. in *Immersion Cooling of Digital Computers, Cooling of Electronic Systems*; Kakac, S.; Yuncu, H.; Hijikata, K., Eds.; Kluwer Academic Publishers: Boston, 1994; pp. 539–621. (b) Mudawar, I.; Maddox, D. E. *Int. J. Heat Mass Transfer* **1989**, *32*, 379–394.

(13) (a) Schmaljohann, D.; Bae, Y. C.; Weibel, G. L.; Hamad, A. H.; Ober, C. K. *Proc. SPIE-Int. Soc. Opt. Eng.* **2000**, *3999*, 330–334. (b) Bae, Y. C.; Dai, J.; Weibel, G. L.; Ober, C. K. *Polym. Prepr.* **2000**, *41*, 1586–1587. (c) Schmaljohann, D.; Bae, Y. C.; Dai, J.; Weibel, G. L.; Hamad, A. H.; Ober, C. K. *J. Photopolym. Sci. Technol.* **2000**, *13*, 451–458. (d) Bae, Y. C.; Ober, C. K. *Polym. Prepr.* **2001**, *42*, 403–404. (e) Bae, Y. C.; Douki, K.; Yu, T.; Dai, J.; Schmaljohann, D.; Koerner, H.; Ober, C. K. *Chem. Mater.* **2002**, *14*, 1306–1313.

(14) See, for instance, Fluoroguard Polymer Additive, Technical Bulletin H-79796-1; DuPont Chemical Solutions Enterprise: Wilmington, 2001.

(15) (a) *Fluorinated Surfactants: Synthesis, Properties, and Applications*; Kissa, E., Ed.; Marcel Dekker: New York, 1994. (b) Moody, C. A.; Kwan, W. C.; Martin, J. W.; Muir, D. C. G.; Mabury, S. A. *Anal. Chem.* **2001**, *73*, 2200–2206.

(16) (a) Hozumi, A.; Takai, O. *Thin Solid Films* **1997**, *303*, 222–225. (b) Jisr, R. M.; Rmaile, H. H.; Schlenoff, J. B. *Angew. Chem., Int. Ed.* **2005**, *44*, 782–785.

(17) Höpken, J. Proefschrift. Ph.D. thesis, Universiteit Twente, Twente, Germany, 1991.

(18) (a) Twieg, R. J.; Russell, T. P.; Siemens, R.; Rabolt, J. F. *Macromolecules* **1985**, *18*, 1361–1362. (b) Rabolt, J. F.; Russell, T. P.; Siemens, R.; Twieg, R. J.; Farmer, B. *Polym. Prepr.* **1986**, *27*, 223–224. (c) Pugh, C.; Höpken, J.; Möller, M. *Polym. Prepr.* **1988**, *29*, 460–461.

(19) Ku, C.-Y.; LoNostro, P.; Chen, S.-H. *J. Phys. Chem. B* **1997**, *101*, 908–914.

(20) Höpken, J.; Pugh, C.; Richtering, W.; Möller, M. *Makromol. Chem.* **1988**, *189*, 911–925.

(21) (a) Krafft, M.-P.; Riess, J. G. *Angew. Chem., Int. Ed. Engl.* **1994**, *33*, 1100–1101. (b) Park, H. K.; Ha, T. H.; Kim, K. *Langmuir* **2004**, *20*, 4851–4858. (c) Aldebert, P.; Guglielmi, M.; Pineri, M. *Polym. J.* **1991**, *23*, 399–406.

(22) Terech, P.; Rodriguez, V.; Barnes, J. D.; McKenna, G. B. *Langmuir* **1994**, *10*, 3406–3418.

(23) (a) Loiseau, J.; Lescanne, M.; Colin, A.; Fages, F.; Verlhac, J.-B.; Vincent, J.-M. *Tetrahedron* **2002**, *58*, 4049–4052. (b) Emmanouli, V.; Choul, M. E.; André-Barrès, C.; Guidetti, B.; Rico-Lattes, I.; Lattes, A. *Langmuir* **1998**, *14*, 5389–5395.

(24) (a) An, B.-K.; Lee, D.-S.; Lee, J.-S.; Park, Y.-S.; Song, H.-S.; Park, S. Y. *J. Am. Chem. Soc.* **2004**, *126*, 10232–10233. (b) Sawada, H.; Kurachi, M.; Maekawa, T.; Kawase, T.; Hayakawa, Y.; Takishita, K.; Tanedani, T. *J. Appl. Polym. Sci.* **1999**, *72*, 1101–1108. (c) Sawada, H.; Nakamura, Y.; Katayama, S.; Kawase, T. *Bull. Chem. Soc. Jpn.* **1997**, *70*, 2839–2845. (d) Da, J.; Hogen-esch, T. E. *J. Polym. Sci. A: Polym. Chem.* **2004**, *42*, 360–373. (e) Da, J.; Hogen-esch, T. E. *Macromolecules* **2003**, *36*, 9559–9563.

(25) Sharp, K. G. *Mater. Res. Soc. Symp. Proc.* **1998**, *520*, 123–135.

(26) JADE, Release 5.0.35 (SPS); Materials Data Inc.: Livermore, CA, 2000.

(27) Stewart, J. J. P. *J. Comput. Chem.* **1989**, *10*, 209–220.

Table 1. Appearance^a and T_g Values (in Parentheses; °C) of Gels Made from FmNHn and FmOHn Gelators in Perfluorinated Liquids

	F11OH3	F7NH18		F11NH3		F11NH4		F11NH6 ^c		F11OH18	
liquid	5 wt %	2 wt %	5 wt %	2 wt %	5 wt %	2 wt %	5 wt %	2 wt %	5 wt %	2 wt %	5 wt %
<i>n</i> -perfluoro-octane	S	jelly	OG (38–42) ^{b,f}	TG (57) ^c	TG (67) ^c	TG (58) ^c	TG (69) ^c	TG (52)	TG (60)	TG (41) ^e	OG (46) ^e
FC-72	S	P	P	TG (46) ^c	TG (56) ^c	TG (45) ^c	TG (52) ^c	TG (54)	TG (62)	TG (38) ^e	OG (46) ^e
FC-77	S	TG (62) ^b	OG (55–58) ^{b,f}	TG (47) ^c	TG (59) ^c	TG (48) ^c	TG (59) ^c	TG (59)	TG (67)	TG (38–40) ^{e,f}	OG (43–46) ^{e,f}
HFE–7500	S	TG (66) ^b	OG (74) ^b	TG (32) ^d	TG (78) ^c	TG (34) ^d	TG (83) ^c	TG (37)	TG (51)	P	TG (33) ^e
FC-43	S	jelly	OG (35–40) ^{b,f}	TG (59) ^c	TG (64) ^c	TG (56) ^c	TG (66) ^c	TG (68)	TG (74–78)	TG (48) ^e	TG (50) ^e
L-18543	S	I	I	TG (39) ^c	TG (51) ^c	TG (41) ^c	TG (48) ^c	TG (51)	TG (53)	P	OG (44) ^e

^a S, solution; P, precipitate; I, insoluble; TG, turbid gel; OG, opaque gel. ^{b–e} Stable for (b) 2 months; (c) > 16 months; (d) 14 months; and (e) > 5 months. ^f Solvent separated on heating.

of Standards and Technology (NIST, Gaithersburg, MD)²⁸ at a wavelength $\lambda = 8.09$ Å and at 15.3, 5.0, and 1.0 m distances with a detector lateral offset of 0.25 m for the 5.0 and 1.0 m distances. The scattering vector range investigated was $0.0011 < |\vec{Q}| < 0.33$ Å⁻¹ ($Q = 4\pi/\lambda \sin \theta/2$, where θ is the scattering angle and λ is the wavelength of the neutrons).

SANS Sample Preparation and Data Analyses. Gel samples with FC-43 or *n*-perfluorooctane as the liquid were prepared in 2 mm path length cylindrical quartz cells. The scattered intensity was corrected for background and parasitic scattering,²⁹ placed on an absolute level using a direct measurement of the beam flux, and circularly averaged to yield the scattered intensity, $I(Q)$, as a function of the wave vector, Q .

The specific contrasts were taken to be $\overline{\Delta b} = -7.253 \times 10^9$ cm g⁻¹ (F11NH6/FC-43), $\overline{\Delta b} = -2.367 \times 10^9$ cm g⁻¹ (F11NH3/*n*-perfluorooctane), $\overline{\Delta b} = -4.489 \times 10^9$ cm g⁻¹ (F11NH3/FC-43), $\overline{\Delta b} = -4.978 \times 10^9$ cm g⁻¹ (F11NH4/FC-43), and $\overline{\Delta b} = -23.717 \times 10^9$ cm g⁻¹ (F7NH18/FC-43). The densities of the gelators F7NH18 ($d_g = 1.16 \pm 0.04$ g cm⁻³) and F11NH6 ($d_g = 1.61 \pm 0.02$ g cm⁻³) in their solid phases were determined at room temperature by weighing a column of each compound that had been melted and solidified to remove air spaces in a capillary tube of known diameter. Densities of the liquids are $d_l = 1.9$ g cm⁻³ for FC-43 and $d_l = 1.766$ g cm⁻³ for *n*-perfluorooctane.³⁰

The methodology for analyses^{31,32} used the cross-sectional radius of gyration R_c , deduced in eq 1 from the slope of low- Q linear variations of $\ln(QI)$ versus Q^2 plots, to calculate the scattering function of cylindrical fibers (eq 2).

$$QI(Q) = QI_0 \exp(-R_c^2 Q^2/2) \quad (1)$$

For cylindrical scatterers $R_c = R_0/\sqrt{2}$. In eq 2, M is the molecular weight of the gelator, N is the Avogadro's number, $\Delta b = \bar{b}_g - \bar{b}_l d_l v_g$ is the specific contrast of the aggregate with \bar{b}_g and \bar{b}_l being the specific neutron scattering length density of the gelator and the liquid, respectively, and v_g is the specific volume of the gelator. R is the radius of the rodlike species of concentration C (g cm⁻³).

$$I(Q) = \frac{\pi C n_L M \Delta b^2}{N Q} \left[\frac{2J_1(QR)}{QR} \right]^2 \quad (2)$$

J_1 is the first-order Bessel function of the first kind. The number of aggregated molecules per unit length of fibers was deduced

(28) Glinka, C. J.; Barker, J. G.; Hammouda, B.; Krueger, S.; Moyer, J. J.; Orts, W. J. *J. Appl. Crystallogr.* **1998**, *31*, 430–445.

(29) NG3 and NG7 30-Meter SANS Instruments Data Acquisition Manual; Cold Neutron Research Facility at the National Institute of Standards and Technology: Gaithersburg, MD, 2002.

(30) (a) Haszeldine, R. N. *J. Chem. Soc.* **1951**, 102–104. (b) Haszeldine, R. N. *Res.* **1950**, *3*, 430–431. (c) Haszeldine, R. N.; Smith, F. *J. Chem. Soc.* **1950**, 3617–3623. (d) Haszeldine, R. N.; Smith, F. *J. Chem. Soc.* **1951**, 603–608.

(31) Glatter, O.; Kratky, O. *Small Angle X-ray Scattering*; Academic Press: London, 1982.

(32) Guinier, A.; Fournet, G. *Small Angle Scattering of X-rays*; Wiley: New York, 1955.

using the extrapolated cross-sectional intensity at low Q , $(QI)_0$ (eq 3).

$$n_L^0 = 10^3 N \frac{(QI)_0}{\pi M^2 p C_0 (\bar{b}_g - \bar{b}_l d_l v_g)^2} \quad (3)$$

p is the fraction of the gelator molecules involved in the spontaneous aggregation reaction. Crystalline gel networks for which the scattering is dominated by large-scale fluctuations between heterogeneities in a random two-phase distribution can be described using the Debye–Bueche model.³³ The spatial correlations of average length Ξ are damped according to the exponential correlation function, $g(r) \cong \exp(-r/\Xi)$, so that the intensity $I(Q)$ is expressed in eq 4.

$$I(Q) \propto \frac{\Xi^3}{(1 + Q^2 \Xi^2)^2} \quad (4)$$

Materials. Syntheses of the LMOGs have been reported previously.⁷ *n*-Perfluorooctane was purchased from PCR Incorporated (Gainesville, FL) and used as received. All other perfluorinated liquids in Chart 2 were a gift from 3M Corporation, St. Paul, MN, and were used without further purification.

Preparation of Gels and Determination of Gelation Temperatures. Weighed amounts of a liquid and a solid were placed in a glass tube (5 mm i.d.) that was usually flame-sealed (to avoid evaporation). Gel samples for POM analyses were prepared in closed Pyrex flattened capillary cells (2 mm path length). The tubes were heated in a water bath (until all solid dissolved) and then cooled rapidly in an ice–water mixture. This procedure was repeated to ensure sample homogeneity. Gelation temperatures (T_g) were determined by the inverse flow method.³⁴ A gel in a sealed glass tube was inverted, strapped to a thermometer near the bulb, and immersed in a stirred water bath at room temperature. The temperature of the bath was raised slowly and the range of T_g was taken from the point at which the first part of the gel was observed to fall to the point at which all had fallen under the influence of gravity.

Results and Discussion

Gelation Studies. Table 1 summarizes the results from our attempts to gelate the six perfluorinated liquids in Chart 2 by 2 and 5 wt % of the LMOGs in Chart 1. Although F11NH3, F11NH4, and F11NH6 were able to gelate all the liquids, their gels and those of the other LMOGs had a turbid or opaque appearance in all cases. In several nonfluorinated liquids, F11NH3, F11NH4, and F11NH6 form transparent gels, indicative of SAFIN networks in which the fibers have very thin cross sections.⁷ Although very similar in structure to amide F11NH3, ester F11OH3 was unable to gelate any of the liquids examined in Table 1. The two molecules differ only in the nature of the ester

(33) Debye, P.; Bueche, A. M. *J. Appl. Phys.* **1949**, *20*, 518–525.

(34) Eldridge, J. E.; Ferry, J. F. *J. Phys. Chem.* **1954**, *58*, 992–995.

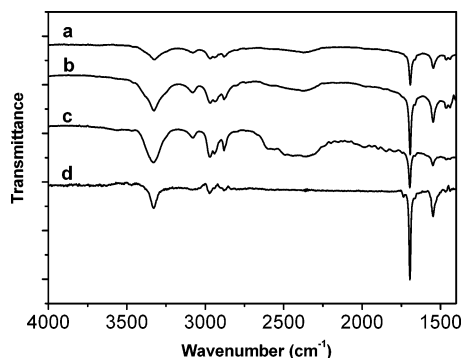


Figure 1. IR spectra of neat solid F11NH3 (a) and its 5 wt % gels in *n*-perfluorooctane (b), FC-43 (c), and HFE-7500 (d). The contributions from the liquids have been subtracted approximately in parts b–d.

or amide group separating the perfluoroalkyl and alkyl groups. The ability of the secondary amide group to act as an H-bond donor and acceptor, whereas dipole–dipole forces are the strongest interactions available between ester groups, must be responsible in large part for the difference between the excellent gelation by F11NH3 and the lack of gelation by F11OH3. Extension of the alkyl chain of F11OH3 to 18 carbon atoms increases the strength of London dispersion forces, allowing aggregates of F11OH18 to gelate some of the perfluorinated liquids. Even then, the longer octadecyl chain of the ester F11OH18 is insufficient to make its perfluorinated liquid gels more stable thermally or temporally than those of the amides F11NH3, F11NH4, and F11NH6.

However, ester F11OH18 is a more efficient gelator of the perfluorinated liquids than amide F7NH18, whose

alkyl chain is also long but whose perfluoroalkyl part is somewhat shorter. At 2 wt %, F7NH18 was able to gelate only FC-77 and HFE-7500, whereas F11OH18 formed gels with 4 of the 6 liquids in Chart 2. Clearly, the strength of the interactions among neighboring perfluoroalkyl chains of these LMOGs within their SAFINs is a very important factor in gel stability *even when the liquid components are perfluorinated*.

IR Spectral Studies. IR peaks characteristic of the carbonyl and amino moieties appear at similar spectral positions in neat powders of the amide LMOGs and their gels (Figure 1, and Supporting Information Figures 1–3); H-bonding is similar in the two phases. For instance, in neat solid F11NH3, F11NH4, and F11NH6 and its *n*-perfluorooctane gels, $\nu_{\text{N-H}} = 3326 \pm 2 \text{ cm}^{-1}$ and $\nu_{\text{C=O}} = 1693 \pm 2 \text{ cm}^{-1}$ (Supporting Information Table 2). However, the widths of NH stretching bands depend on both the LMOG and liquid, indicating that the distribution of H-bonds is different in different gels.

Polarizing Optical Microscopy (POM). Unlike gels formed in nonfluorinated liquids,⁷ these are turbid in appearance and birefringent, indicating a more ordered molecular arrangement within the aggregates of the SAFINs. Optical micrographs of gels containing 5 wt % LMOG in *n*-perfluorooctane, FC-43, and HFE-7500 are shown in Figures 2 and 3 and Supporting Information Figures 4–6. The appearances of the SAFINs in the micron distance range depend strongly on the gelator and, to a lesser extent, the liquid. Since the appearance of a SAFIN can be very dependent on the procedure for cooling the sol phase below T_g ,³⁵ all of these gels were prepared by the same cooling protocols (see Experimental Section). As examples, amides F11NH3, F11NH4, and F11NH6 form

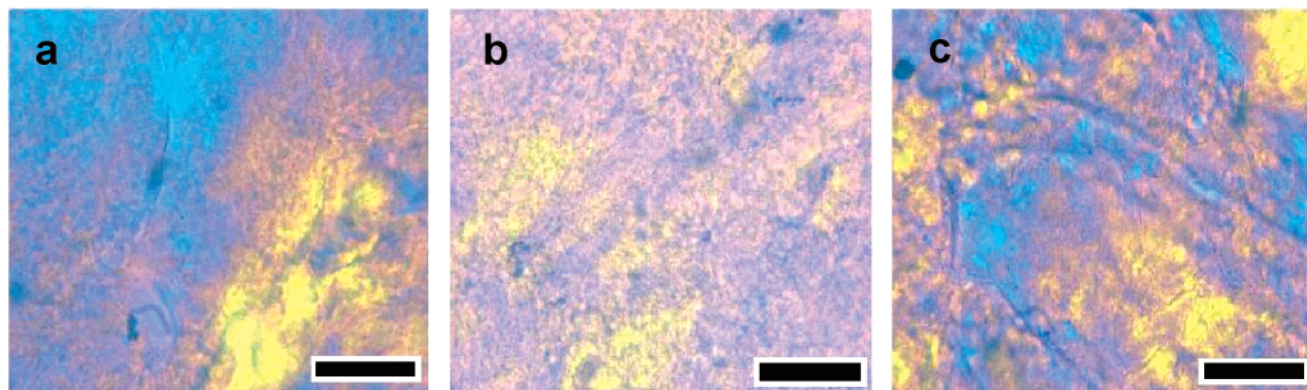


Figure 2. Polarizing optical micrographs (room temperature) of 5 wt % F11NH3 in (a) FC-43, (b) HFE-7500, and (c) *n*-perfluorooctane. Black space bars are 200 μm . The images were taken with a full-wave plate.

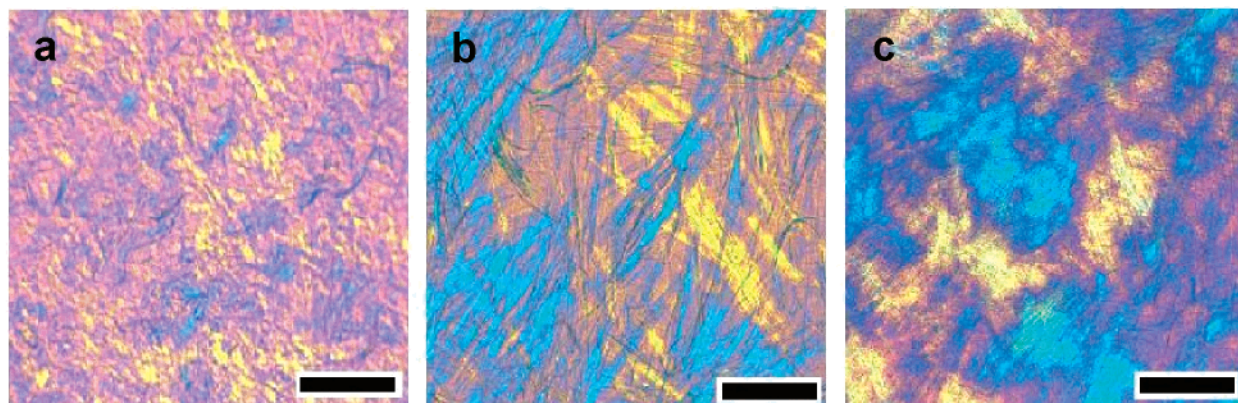


Figure 3. Polarizing optical micrographs (room temperature) of 5 wt % F11OH18 in (a) FC-43, (b) HFE-7500, and (c) *n*-perfluorooctane. Black space bars are 200 μm . The images were taken with a full-wave plate.

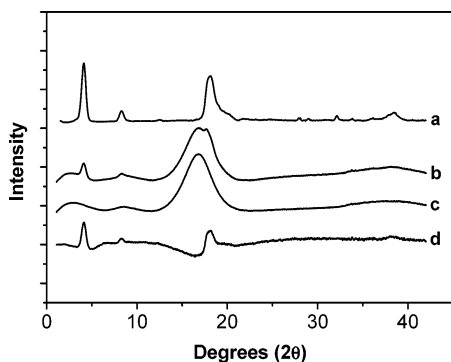


Figure 4. X-ray diffraction patterns (room temperature) of F7NH18: (a) powder; (b) 5 wt % gel in FC-43; (c) neat FC-43; and (d) diffractogram b – diffractogram c.

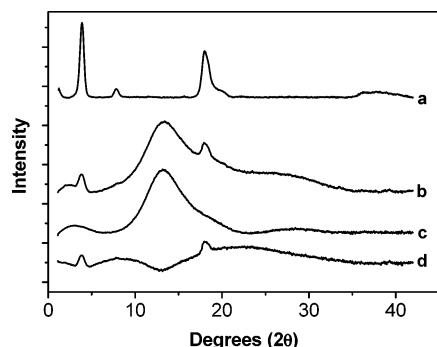


Figure 5. X-ray diffraction patterns (room temperature) of F11NH4: (a) powder; (b) 5 wt % gel in HFE-7500; (c) neat HFE-7500; and (d) diffractogram b – diffractogram c.

shorter aggregates than F11OH18 whose bundles of fibers are ~ 100 – $200\ \mu\text{m}$ in length. High aspect ratios of the fibers indicate that their formation involves a very anisotropic growth process.

F7NH18 also forms shorter aggregates (Supporting Information Figure 4) but they are not as evenly distributed as in the case of F11NH3, F11NH4, and F11NH6. The poor gelating ability of F7NH18 must be related to the aggregation and uneven distribution of its birefringent fibers. Based on comparisons of the optical micrographs of gels of ester F11OH18 and of the amides, the shorter aggregates of the latter, irrespective of the liquid employed, are attributed to the additional attractive intermolecular interactions allowed by H-bonding within the fibers. These qualitative observations will require additional investigation to determine the link between fiber growth and the strength of the intermolecular LMOG interactions.

X-ray Diffraction Studies. The X-ray diffraction peaks of the assemblies of gels containing 5 wt % FmX_Hn in different liquids were obtained by subtracting the “amorphous scatter” of the liquid components from the total gel diffractograms (Figures 4–6 and Supporting Information Figures 7–11),³⁶ and they are compared with diffraction patterns of the neat powders. Although the POM of each of the gels provides no evidence for nonfibrillar LMOG crystallites, they could, if present, contribute to or be totally responsible for the observed diffractions.

Despite the weakness of some diffraction peaks from the gels, their positions generally coincide with peaks from

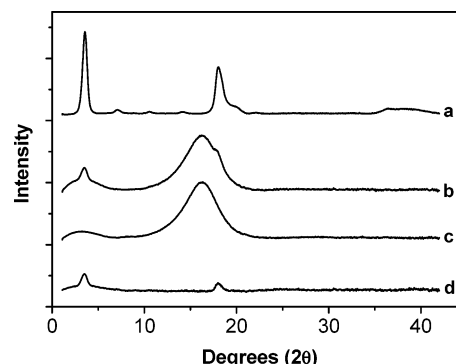


Figure 6. X-ray diffraction patterns (room temperature) of F11NH6: (a) powder; (b) 5 wt % gel in *n*-perfluorooctane; (c) neat *n*-perfluorooctane; and (d) diffractogram b – diffractogram c.

Table 2. Lamellar Spacings (*d*) from the Lowest Angle Peaks in X-ray Diffraction Patterns of Neat Powders of FmX_Hn, Their 5 wt % Gels in *n*-Perfluorooctane, and Calculated Extended Molecular Lengths

LMOG	extended molecular length (Å)	<i>d</i> (Å)	
		powder	gel
F7NH18	36.5	56.4	56.8
F11NH3	23.9	21.4	21.4
F11NH4	25.2	22.6	22.3
F11NH6	27.7	24.8	25.1
F11OH18	42.7	67.6	65.1

the neat powders; the molecular packing arrangements of the gel assemblies and the bulk crystals are the same.³⁶ However, diffraction peaks in the high-angle region from aggregates of F11OH18 in gelated HFE-7500 and from the neat powder have different positions in 2θ (Supporting Information Figure 11). In fact, it is more common for LMOGs in gel assemblies and their neat solids to pack differently.^{1,36,37} Diffractograms of all of the LMOGs as neat powders and in gels possess a low-angle peak (and, in some cases, higher order diffractions of it) that is consistent with lamellar organizations within the SAFIN fibers. Lamellar packing has been proposed for gelator networks of the diblock molecule, heptadecafluorotetracosane (F8H16), as well.^{19a} The layer thicknesses in the fibers of our gel phases (*d*) have been calculated from the low-angle peaks using Bragg’s law (Table 2), and they are the same as in the neat solid phase of the gelator even for F11OH18 (where the intralayer packing arrangement in the gel and neat solid phases differs!).

The *d* values depend primarily on the lengths of the alkyl and perfluoroalkyl chains of these LMOGs, and they need not correspond to an extended molecular length when the length of the alkyl chain portion is very long.⁷ Thus, the experimental *d* values of F7NH18 and F11OH18 are about 50% longer than the calculated molecular lengths in the most extended conformations,³⁸ and the layers must be interdigitated.⁷ When the alkyl chains are shorter, as in F11NH3, F11NH4, and F11NH6, the *d* values are consistently only slightly smaller than the calculated

(35) (a) Lescanne, M.; Grondin, P.; d’Aléo, A.; Fages, F.; Pozzo, J.-L.; Mondain Monval, O.; Reinheimer, P.; Colin, A. *Langmuir* **2004**, *20*, 3032–3041. (b) Abdallah, D. J.; Weiss, R. G. *Chem. Mater.* **2000**, *12*, 406–413. (c) Huang, X.; Terech, P.; Raghavan, S. R.; Weiss, R. G. *J. Am. Chem. Soc.* **2005**, *127*, 4336–4344.

(36) Ostuni, E.; Kamaras, P.; Weiss, R. G. *Angew. Chem., Int. Ed. Engl.* **1996**, *35*, 1324–1326.

(37) (a) Lin, Y.-C. Ph.D. Thesis, Georgetown University, Washington, DC, 1987. (b) Lin, Y.-C.; Kachar, B.; Weiss, R. G. *J. Am. Chem. Soc.* **1989**, *111*, 5542–5551. (c) Lin, Y.-C.; Weiss, R. G. *Macromolecules* **1987**, *20*, 414–417. (d) Mukkamala, R.; Weiss, R. G. *Chem. Commun.* **1995**, 375–376. (e) Mukkamala, R.; Weiss, R. G. *Langmuir* **1996**, *12*, 1474–1482. (f) Lu, L.; Weiss, R. G. *Langmuir* **1995**, *11*, 3630–3632. (g) Furman, I.; Weiss, R. G. *Langmuir* **1993**, *9*, 2084–2088.

(38) Calculated by Hyperchem (version 5.1) molecular modeling system at the PM3 level, adding the van der Waals radii of the terminal atoms. *Lange’s Handbook of Chemistry*, 13th ed.; Dean, A. J., Ed.; McGraw-Hill: New York, 1985; Sect. 3, pp 121–126.

Table 3. Neutron Scattering Features of Gels Consisting of FmNHn in Perfluorinated Liquids at Different Concentrations^a

LMOG	liquid	wt % (C, g cm ⁻³)	category	peak (Å ⁻¹)	$\langle d \rangle$ (Å)	R_c (Å)	R_0 (Å)
F11NH3	FC-43	1 (0.019)	I	0.290	21.7	137	194
F11NH4	FC-43	1 (0.019)	I	0.278	22.6	115	162
F11NH6	FC-43	2 (0.038)	I	0.249	25.2	144.5	204
F7NH18	FC-43	1 (0.019)	II	0.109, 0.213	57.6, 29.5		
F11NH3	<i>n</i> -perfluorooctane	1 (0.017)	II	0.285	22.05		

^a The categories of scattering are described in the text. Bragg peak positions and corresponding real-space distances are indicated, along with cross-sectional radii of gyration R_c and the deduced geometrical radii R_0 for a cylindrical morphology.

extended molecular lengths and molecules within a layer must be oriented (nearly) normal to their layer planes.⁷

Small-Angle Neutron Scattering (SANS) Studies.

The SANS technique uses the Fourier transform of large scale neutron scattering length density fluctuations³² in a system. SANS has been demonstrated to be able to characterize the structures of nanoparticles in a dispersing medium, and, in particular, SAFINs in molecular gels.³⁹

Most networks that form the solid component of LMOG gels are comprised of rigid fiberlike species interconnected where fibers merge or bundle.¹ Analyses of SANS data are based on the assumption that scattering is due mainly to the form-factor contribution of fibrillar species at the low LMOG concentrations used. Increasing its concentration enhances the volume proportion of nodal zones and, as a result, the intensity of Bragg peak(s) arising from the molecular ordering in the fibers and bundles of more crystal-like networks. The *N*-alkyl perfluoroalkanamides investigated here exhibit two types of scattering patterns that depend on the nature of the LMOG and the perfluorinated liquid (Table 3).

Category I scattering is typical of gels with SAFINs in which the form-factor scattering of the individual fiberlike components can be distinguished. Under this condition, a linear part in a $\ln(QI)$ versus Q^2 plot enables the extraction of a radius of gyration R_c value for the cross section of the fibers (eqs 1 and 2). The value is comparable to that obtained from a fit of a calculated scattering function using eqs 1 and 2 in the largest experimental Q range. The modeling under such single-particle conditions usually excludes the innermost part of the scattering curve, where extra scattering from the nodal zones of the SAFIN as well as the large- Q domain whose Bragg peaks can characterize its crystallinity. Equation 3 is also used to take advantage of calibrated intensities and estimate the typical aggregation number of the sections of fibers and the prefactor of eq 2 expressed in absolute units.

Category II scattering for the FmNHn is characterized by a low- Q Q^{-4} decay followed by Bragg diffraction peak(s). This scattering is masked by the signals from large aggregates in both the low and large- Q regions. The low- Q part of the scattering signal can be attributed to large-scale fluctuations in a random two-phase distribution as described by the Debye–Bueche model (eq 4).³³ Such heterogeneities are the nodal zones of the SAFIN in which fibers merge. They ensure the connectivity over an infinitely large length scale and participate to viscoelastic behaviors typical of strong gels with significant yield stress values. At large angles, Bragg peak(s) reveal the periodicities of diffracting planes existing in the bundles or nodal zones of the SAFIN.

The organogel of F11NH6 (as well as those of F11NH3 and F11NH4) in FC-43 is representative of category I scatterers. A radius of gyration $R_c = 144.5$ Å for the cross section of fibrillar species can be extracted from a plot

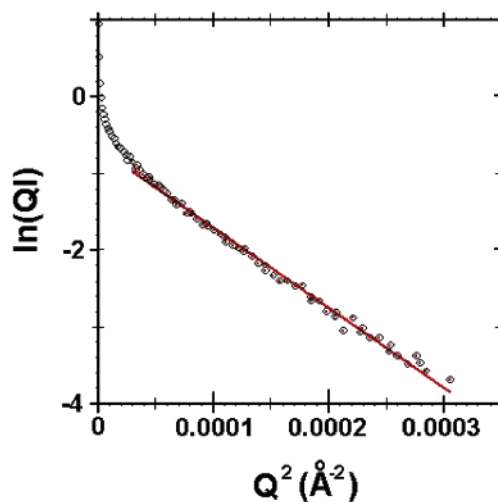


Figure 7. Determination of the cross-sectional radius of gyration R_c for a F11NH6/FC-43 organogel (2 wt %; $C = 0.038$ g cm⁻³). The low- Q upturn is due to the contribution from nodal zones of the crystal-like SAFIN.

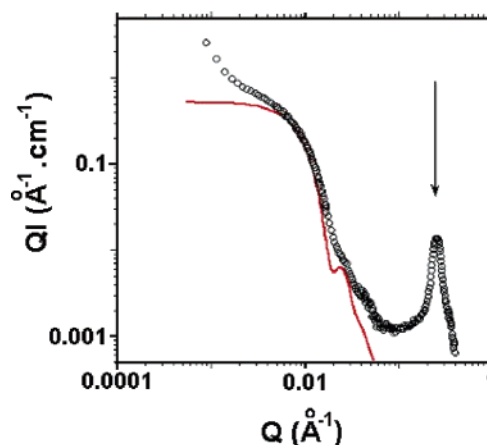


Figure 8. Experimental (○) cross-sectional intensity versus Q curve for a F11NH6/FC-43 organogel (2 wt %; $C = 0.038$ g cm⁻³). The full line is a calculated form-factor scattering function for cylinders with $R_0 = 200$ Å. The arrow points to a Bragg peak at $Q = 0.249$ Å⁻¹.

$\ln(QI)$ versus Q^2 (Figure 7). For a cylindrical symmetry of the aggregates, it corresponds to $R_0 = 204.3$ Å. This value can be compared with the theoretical scattering form-factor function using expression 2 and shown in Figure 8. The scattering calculated for $R_0 = 200$ Å describes well the experimental profile, including the first form-factor oscillation, indicating that the F11NH6 fibers exhibit rather monodisperse sections. The R_0 value is also similar to that extracted from R_c and provides additional support for the cylindrical cross-section hypothesis. Deviations of the fit at very low Q values in Figure 7 are assumed to be due to the extra scattering from nodal zones of the SAFIN. An intense Bragg peak at $Q = 0.249$ Å⁻¹

(39) Terech, P.; Volino, F.; Ramasseul, R. *J. Physique* **1985**, *46*, 895–903.

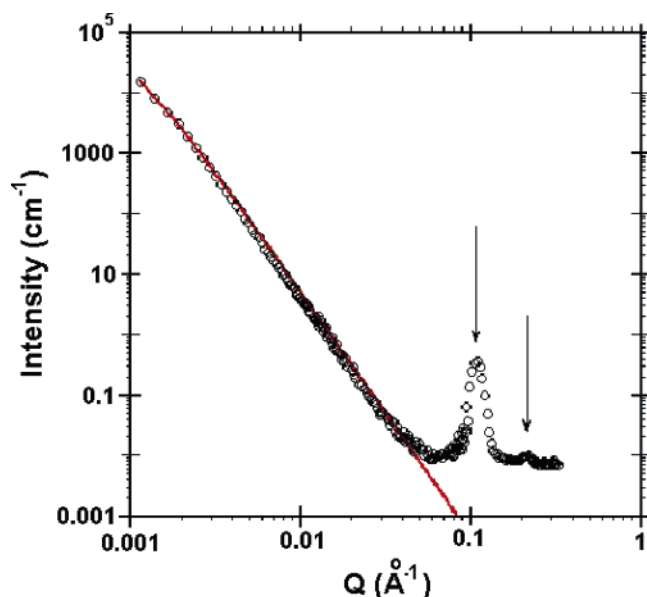


Figure 9. Experimental (○) scattering intensity versus Q curve for a F7NH18/FC-43 organogel (1 wt %; $C = 0.019 \text{ g cm}^{-3}$). The straight line is a fit according to eq 3, from which the average distance between nodes, 1400 Å, can be deduced.

($\langle d \rangle = 25.2 \text{ Å}$) confirms the crystallinity of the network. Diffracting planes involve periodicities corresponding to extended molecular distances (Table 3) consistent with head-to-tail molecular arrangements. The extrapolated value, $(QI)_0$, is used to deduce $n_L \sim 71 \text{ molecules Å}^{-1}$, the number of aggregated molecules per unit length of fiber. Depending on the mechanism of molecular stacking in the fibers, the axial repeat unit d_{ax} along the fiber axis can be either a side-by-side short distance (of the order of ca. 4.5 Å) or, as indicated by the X-ray diffraction results, proportional to the extended molecular length. The case of molecules whose long axes are parallel to the fiber axis would not lead to fibers with rather monodisperse sections. Assuming the long axes of the molecules are radially distributed within the fibers, about 320 molecules would compose the basic sectional unit. Figure 8 presents the theoretical scattering in absolute units using the prefactor defined in eq 2 with the calculated value $\overline{\Delta b}$ and the estimated value of n_L . Considering the different sources of imprecision [N.B., experimental density values, presence of a fraction of molecules existing in a solubilized “monomeric” state in the gel phase, uncertainty in estimates using calibrated intensities, complexity of the structural composition of bundles of fibers constituting the SAFINs, and the balance between amplification and compensation of these uncertainties (eq 2)], we consider the agreement to be satisfactory.

A gel of 1 wt % (0.019 g cm^{-3}) F7NH18 in FC-43 exhibits features typical of a category II scatterer (Figure 9). A clear Q^{-4} intensity decay is present while Bragg peaks at $Q = 0.109$ ($\langle d \rangle = 57.6 \text{ Å}$) and 0.213 ($\langle d \rangle = 29.5 \text{ Å}$) confirm the crystalline nature of the SAFIN. Analysis of the low- Q part according to a random two-phase distribution (eq 4) gives a mean correlation distance (Ξ) between the nodal heterogeneities of about 1400 Å. From $\Delta Q = 0.0175 \text{ Å}^{-1}$ (the width at half-height of the Bragg peak at $Q = 0.109 \text{ Å}^{-1}$), the average size of the diffracting crystallites is about 2400 Å.⁴⁰ Interfacial scattering of such large aggregates accounts for the Q^{-4} intensity decay noted

above. The ratio of $\langle d \rangle$ spacings of the two Bragg peaks, 1:1.95 ($\approx 1:2$), suggests parallel stacking of the fibers in lamellar-like bundles. The shorter and longer spacings appear related to the single and double extended molecular length of F7NH18, 36.5 Å, and indicate a tail-to-tail packing mode with either conformational bending or, as suggested above, some interdigitation. A major structural distinction between F11NH3, F11NH4, and F11NH6 (that pack in head-to-tail fashions within their SAFINs) and F7NH18 is the lengths of the alkyl chains. Based on the (admittedly limited) data in hand, it appears that tail-to-tail packing requires the longer alkyl chains.

Conclusions

Thermally and temporally stable organogels can be prepared from a wide variety of perfluorinated liquids and small concentrations of *N*-alkyl perfluoroalkanamide LMOGs. The dependence of the structural features of the SAFINs at several length scales on their constituent LMOG molecules and the specific perfluorinated liquid has been explored. Surprising nuances in the SAFIN structures are manifested in the gel stabilities. The robustness of the gels depends on several structural factors of the LMOGs, including the lengths of the alkyl and perfluoroalkyl chains and the ability of the secondary amide group to enter into intermolecular H-bonding arrangements. The latter is apparent from studies conducted with esters analogous to the amides and from information in the literature employing diblock perfluoroalkylalkanes (i.e., molecules such as our FmX_nH_n but lacking the X group that separates the perfluoroalkyl and alkyl molecular segments).^{17–20} The incompatibility of the alkyl and perfluoroalkyl units produces supramolecular aggregates that are stabilized further by H-bonding among amide groups and, to a lesser extent, by dipolar interactions among carbonyl groups.

The packing of LMOGs in their neat solid phases and SAFINs appear to be the same in most of the cases explored. The distance d that defines the layer thicknesses depends acutely on the length of the alkyl chain of the FmX_nH_n. Both X-ray scattering and SANS measurements demonstrate that d changes from being near an extended molecular length in the LMOGs with shorter alkyl chains to about 1.5 times the length when a longer (octadecyl) chain is present. Where comparisons are possible, the d values obtained from the X-ray and SANS methods are in good agreement. Empirically, when the lamellar thickness of a SAFIN corresponds to about 1.5 times the extended molecular length, as for F11OH18 and F7NH18, the gels are less stable than when d is near the extended molecular length.

The SANS measurements reveal head-to-tail packing within lamellae of F11NH_n/FC-43 gels when $n < 7$, and tail-to-tail packing in F7NH18/FC-43 and F11NH3/*n*-perfluorooctane gels. The cross-sectional dimensions of the F11NH_n and F7NH18 fibrils in the perfluorinated liquids are very small (in the nanometer range) and depend on the length of the alkyl chain. It is interesting to note that the cross sections of the fibers from one LMOG are much narrower in gels of perfluorinated liquids than in nonfluorinated liquids.⁷ Although we have not investigated the origin of these differences here, they may derive from factors associated with the kinetics of the gelation process^{35c,41} or the energetics of surface interactions between fibrils and the liquid.⁵ It is a point of interest

(40) Guinier, A. *X-ray Diffraction in Crystals, Imperfect Crystals, and Amorphous Bodies*; Lorrain, P., Lorrain, D. S.-M., translators; W. H. Freeman: San Francisco, 1963.

(41) (a) Terech, P. J. *Colloid Interface Sci.* **1985**, *107*, 244–255. (b) Liu, X. Y.; Sawant, P. D. *Adv. Mater.* **2002**, *14*, 421–426. (c) Liu, X. Y.; Sawant, P. D. *Appl. Phys. Lett.* **2001**, *19*, 3518–3520.

here and one that merits additional attention in order to understand better the SAFINs of many other LMOG gels.

Because these LMOGs are able to gelate a wide variety of fluorinated liquids, including those with additional functional groups, their gels may be useful delivery agents of highly fluorinated reagents for several applications.^{11–15} In addition, they may be a useful vehicle to transport molecular oxygen for synthetic and physiological purposes.⁴² From a fundamental standpoint, these gels present an additional scientific challenge to those interested in how self-assembly leads to objects with very high aspect ratios and low dispersion cross sections. To date, most studies of this sort have focused on hydrophobic/

hydrophilic and lipophobic/lipophilic interactions;^{1f} additional ones operate here.

Acknowledgment. Financial support to the Georgetown group from the National Science Foundation is greatly acknowledged. We thank Dr. Michael Costello of 3M Specialty Fluids, St. Paul, MN, for supplying several of the perfluorinated liquids and The National Institute of Standards and Technology, U.S. Department of Commerce, for providing the neutron research facilities used in this work. We also acknowledge the CNRS for a binational travel grant to P.T.

(42) (a) Riess, J. G. *Artif. Cells, Blood Substitutes, Biotechnol.* **2005**, 33, 47–63. (b) Ju, L. K.; Lee, J. F.; Armiger, W. B. *Biotechnol. Bioeng.* **1991**, 37, 505–511. (c) Pozzi, G.; Montanari, F.; Rispen, M. T. *Synth. Commun.* **1997**, 27, 447–452. (d) Betzemeier, B.; Knochel, P. In *Modern Solvents in Organic Synthesis*; Knochel, P., Ed.; Springer: Berlin, 1999; Vol. 206, pp 61–78. (e) Constantino, M. L. *Int. J. Artif. Organs* **1996**, 19, 284–290.

Supporting Information Available: IR spectra, POM images, table of IR frequencies, and XRD patterns of several gels and neat powder samples. This material is available free of charge via the Internet at <http://pubs.acs.org>.

LA050371Z